SUPPLEMENTARY INFORMATION

Quantifying the effect of PEG length on nanoparticle ligand availability using DNA-PAINT

Teodora Andrian,[a] Silvia Pujals*[a] and Lorenzo Albertazzi*[a,b]

a Institute for Bioengineering of Catalonia (IBEC). The Barcelona Institute of Science and Technology, Baldiri Reixac 15-21, 08028 Barcelona, Spain
b Department of Biomedical Engineering, Institute for Complex Molecular Systems (ICMS), Eindhoven University of Technology, 5612AZ Eindhoven, The Netherlands

Experimental section

Materials

Poly(lactide-co-glycolide)-methoxy-poly(ethylene glycol) GCW301 (Mw PLGA:PEG, 30:1 kDa, L:G in PLGA 50:50) was supplied from GenoTech. Poly(lactide-co-glycolide) AP082 acid endcap (PLGA, 50:50 LA:GA, Mw 25-35 kDa) and poly(lactide-co-glycolide)-poly(ethylene glycol) AK102 (Mw PLGA:PEG 30:5 kDa, L:G in PLGA 50:50) were purchased from PolySciTech. Poly(D,L-Lactide-co-glycolide)-poly(ethylene glycol)-Maleimide SKU 2794 (Mw PLGA:PEG:Maleimide 20:5:0.09707 kDa) was purchased from Nanosoft Biotechnology LLC. Tris(2-carboxyethyl) phosphine hydrochloride (TCEP, 0.5 M, pH 7.0) and Amicon Ultra-4 filters (regenerated cellulose, 100 kDa) were supplied from Merck Life Sciences. Acetonitrile (HPLC grade) was purchased from Carlo Erba Reagents.
Thiol-modified DNA strands (docking strands 1) and Atto647N-labelled DNA strands (imager strands 1 and 3) were designed and purchased from Integrated DNA Technologies. Docking strand 1 and imager strand 1 were used for DNA-PAINT imaging and qPAINT quantification of PLGA-PEG NPs, whilst docking strand 1 and imager strand 3 were used for control experiments. DNA strands were dissolved and stored in sterile TE buffer and used fresh. The DNA strands used have the following DNA sequences, and only 9 bases contribute to hybridization:
Docking strand 1: 3'ATC TAC ATA TT/thiol
Imager strand 1: 5'-CTA GAT GTA T/Atto647N/-3'
Imager strand 3: 5'-GTA ATG AAG A/Atto647N/-3'
Sterile phosphate-buffered saline PBS buffer pH = 7.4 was used for sample preparation. Buffer B which consists of 5 mM Tris-HCl, 10 mM $MgCl_2$, 1 mM EDTA, 0.05% Tween-20 pH=8 was used to dilute imager strands for DNA-PAINT imaging.

Nanoparticle formulation

PLGA-PEG NPs were formulated via the precipitation-solvent evaporation (nanoprecipitation) method according to literature[1] and to our previously reported data[2]. Briefly, 5 mg of polymers and 1.1 mM DiI (reference dye) were dissolved in 500 mL acetonitrile at room temperature. $PLGA_{25\text{-}35k}$ polymer was maintained at a ratio of 15% and mixed with $PLGA_{30k}$-PEG_{5k} (long PEG) or $PLGA_{30k}$-PEG_{1k} (short PEG) and $PLGA_{20k}$-PEG_{5k}-Maleimide polymers at alternating concentrations (10-100%). For example, for the PLGA-PEG 30% maleimide (PEG_{5k}) formulation: 75.0 mL PLGA from stock 10 mg/mL (0.75 mg), $PLGA_{30k}$-PEG_{5k} 152.8 mL from stock 18 mg/mL (2.75 mg), 100.0 mL $PLGA_{20k}$-PEG_{5k}-Maleimide from 15 mg/mL stock (1.5 mg) and 4.5 mL DiI from stock 10 mM (1.1 mM) were dissolved and made up to 500 mL with acetonitrile. The polymer solution was stirred at 200-300 rpm with a magnetic stirrer whilst miliQ water was pipetted at a 1:10 ratio (500 mL polymer solution is pipetted into 5 mL miliQ water). Solvent extraction (evaporation) continued for 5 h under in a fume cupboard at room temperature. NPs were centrifugated and collected (Avanti J-26 XPI, rotor JA-14) using Amicon Ultra-4 filters according to manufacturer's instructions for 10 min at 5,000 x g at 20°C with miliQ water. NPs were stored in miliQ water at 10 mg/mL concentration at 4°C until further use. For the control PLGA-PEG (PEG_{5k}) formulation, no $PLGA_{20k}$-PEG_{5k}-Maleimide was added, the PLGA ratio was maintained at 15%, and $PLGA_{30k}$-PEG_{5k} was increased to 85%. For the control PLGA-PEG (PEG_{1k}) formulation, no $PLGA_{20k}$-PEG_{5k}-Maleimide was added, however it was replaced with $PLGA_{30k}$-PEG_{5k}, whilst the PLGA ratio was maintained at 15%, and $PLGA_{30k}$-PEG_{1k} varied depending on the formulation.

Conjugation to functional ligands (docking strands)

In order to remove the protective disulphide bonds on the thiol group of the docking strands, the reducing agent TCEP was used at a 10:1 molar excess compared to thiol[3]. Briefly, for a PLGA-PEG 30% maleimide formulation, 2.6 μL of 0.5 M TCEP and 116.6 μL of 1.1 mM thiol-docking strand were added to 380.9 μL PBS (pH=7.4) and allowed to stir for 20 min at room temperature. To prevent the re-formation of disulphide bonds[3], argon gas was bubbled inside the glass vial before closing the lid. Then, optimal conjugation was achieved by using a 3:1 molar ratio of thiol to maleimide. During the conjugation process, 500 μL of 10 mg/mL NP stock was added to the solution and mixed for an extra 2 h in the absence of oxygen. Unconjugated docking strands were separated via centrifugation using Amicon Ultra-4 filters as per filter instructions for 10 min at 5,000 x g (rcf) at 20°C with filtered miliQ water. NPs were stored in miliQ water at a concentration of 10mg/mL in the dark at 4°C.

DNA-PAINT chamber preparation

A 40 μL volume flow chamber was assembled from a glass microscopy slide (FisherBrand) and a coverslip (Corning Cover Gass, thickness 1 ½, 22 x 22mm), attached by double-sided tape. Prior to assembly, the coverslips were cleaned first with acetone, then with ethanol 96% for 10 min each by bath sonication, then dried under nitrogen flow. This process removes impurities and improves the NP retention on the coverslip. A 1000x dilution in PBS of the 10mg/ml NP stock was pipetted into the chamber, which was then turned upside down and allowed to adsorb for 20 min. PBS promotes the adsorption of NPs. Unattached NP were washed away with Buffer B. Finally, the chamber was filled with imaging buffer solution (Imager strand diluted in Buffer B to the required concentration) and sealed with nail varnish to avoid evaporation. An imager concentration of 5 nM and 2.5 nM was used for $PLGA_{30k}$-PEG_{5k} and $PLGA_{30k}$-PEG_{1k} respectively.

DNA-PAINT imaging

Imaging was carried out with a Nikon N-STORM system configured for total internal reflection (TIR), using a Perfect Focus System (PFS). Atto647N-Imager strand signal was collected using the 647 nm (160 mW) laser at 60% laser power and the DiI drift correction signal using the 561 nm laser (80 mW) at 2% laser power. No UV activation was required. Fluorescence was collected using a Nikon 100x, 1.49 NA oil immersion objective and passed through a quadband pass dichroic filter (97335 Nikon). Images were acquired onto a 256 x 256-pixel region (pixel size 0.16 μm) of a Hamamatsu ORCA Flash 4.0 camera at 70 ms integration time. For the Atto647N-Imager strand 20,000 frames were acquired in the 647 channel and for the drift correction one frame was acquired every 100 frames in the 561 channel. The time taken for each image acquisition was ~ 25 min.

DNA-PAINT analysis

DNA-PAINT analysis on NPs was previously described by our group[4,5]. Briefly, A Matlab script was used to count the number of localizations in the 647 channel and the 561 (DiI-fiducial marker) channel from the x,y,t coordinates of the txt files. Firstly, the localization clusters from the fiducial 561 channel were identified using a mean-shift clustering algorithm. These clusters were used to identify the center of each individual NP. A second filter was applied allowing the user to manually select specific parameters such as maximum size/minimum localizations per NP to filter out noise/aggregates/elongated shapes. In this case, the manually selected parameters were: minimum points=10, bandwidth=50, maximum particle diameter=160. Then, the localizations from the 647 channel found within a distance of 160 nm from the center of the NP were detected, and then the number and x,y,t coordinates of the localizations and diameter were calculated for each NP. The radius of each NP was estimated as the distance from the mass center making up 90% of the cluster localizations.

Drift Correction

This parameter was previously described in detail by our group[4,5]. Briefly, DiI was encapsulated within PLGA-PEG NPs as it is spectrally different to the dye used on the imager strand, allowing two channel acquisition for two reasons: 1) it allows the correction of the mechanical drift during image acquisition, 2) since the DiI dyes labelling the same NP are simultaneously emitting upon photoexcitation, the resulting clusters of DiI localizations in the reconstructed image correspond, with an uncertainty of a few tens of nm, to the center of the NP. This is an important parameter for further analysis, especially when few docking strands are available on the NP surface. Finally, the amount of DiI dyes per NP is rather low and there is no evidence that it significantly affects the docking−imager interaction. Thanks to the emission of DiI, the NPs themselves acted as subdiffraction-sized fiducial markers for the correction of the mechanical drift, without the need for introduction of additional probes. The low frequency (100 times lower than for imager strand excitation) and power of DiI excitation ensured negligible bleaching of the dyes during image acquisition. To obtain the multicolor images found in Fig. 1 and Fig. 2, the drift-

corrected one-color images of the same field-of-view, acquired using different imager strands, were merged and aligned using ImageJ software, using the clusters of DiI localizations to align the centers of the single NPs.

qPAINT analysis

Data analysis for qPAINT on NPs was previously described by our group[4,5]. Briefly, the x,y,t coordinates of 647 localizations belonging to each NP was analyzed in Matlab using a mean-shift cluster algorithm whereby the diameter and number of localizations was analyzed for each NP. A binary intensity versus time trace was created for each NP, assigning a value of 0 to the frames with 0 localizations and a value of 1 to the frames with one localization. The individual dark times were calculated for each NP, acquiring the corresponding CDF, then fitted with the exponential model and the value of the mean dark time τd* was extracted. The number of ligands per NP was quantified using the equation $n=(k_{ON}c_i\tau_{d^*})^{-1}$ using k_{ON} to be 2.3 x 10^6 M^{-1} s^{-1} as previously calculated on PLGA-PEG NPs[2], and the known imager concentration, of 5 nM for PLGA-PEG (PEG_{5k}) NPs and 2.5 nM for PLGA-PEG (PEG_{1k}). Furthermore, linking is performed using the Nikon software, such that localizations in the very same position that are detected in 10 consecutive frames are counted as 1, while longer are rejected. Thus, if a binding event lasts longer than 1 frame and less than 10 it is counted as one. This affects ON-times but does not affect dark times and qPAINT.

TEM imaging

An in-house carbon-coated copper TEM grid (CF200-CU, 200 mesh, Electron Microscopy Sciences) was first treated using UV glow discharge for 30s using BAL-TEC CTA 005 Glow Discharge Unit to improve the attachment of NPs. Using a fine tweezer, the grid was placed on top of a 40 µL drop of NP solution (2mg/mL) (10mg/mL diluted x5 in MiliQ water) for 3 min for NP attachment. Please note NP solution was vortexed well before attachment to the grid to avoid aggregates. Then the grid was washed to remove impurities and unattached NPs on 40 µL MiliQ water drops for 1 min, 30 sec and 30 sec, then negatively stained using filtered uranyl acetate 2% (UA 2%, in MiliQ water) for 1 min. Excess UA was removed by tapping the edge of the grid on Whatman filter paper. The grid was then allowed to dry overnight in a desiccator. Next, the grid was imaged using a Jeol 1010 (Gatan, Japan) from the Electron Cryomicroscopy Unit from the CCiTUB, equipped with a tungsten cathode. Images were acquired at 80kV with a CCD Megaview 1k x 1k, with a magnification of x20 000-50 000. The NPs diameter was measured using ImageJ software.

Calculations for Table 1 and Table S2, as described in our previous work[6]:

Calculation of Conjugation Efficiency (CE%)

After conjugation of PLGA-PEG NPs to 3-fold molar excess of docking strands, the NP solution was spun down via centrifugation using a bench-top centrifuge (Eppendorf Microcentrifuge 5415 R Sigma-Aldrich) for 20 min at 16.1 x g (rcf) at 20°C leading to a NP pellet formation. The supernatant was collected, then spun down again and the process was repeated for 2 times more to the resulting supernatant until no pellet was observed. The negative control consisted of PLGA-PEG NPs (no maleimide) undergoing the conjugation process and centrifugation steps identically to the test NPs. The final supernatant solutions were analyzed using a NanoDrop ND-1000 Spectrophotometer (at 260 nm) and the CE % was calculated as:

$$\left(1-\frac{Thiol-oligo\ in\ Test\ supernatant\ (abs)}{Thiol-oligo\ in\ Control\ supernatant\ (abs)}\ x\ 3\right) x\ 100\% \quad \text{(Equation 1)}$$

Where x 3 denotes the 3-fold molar excess of docking strands compared to maleimide content.

Calculation of theoretical maleimide groups per NP:

Based on Spherotech's instructions[7]:

Calculating the number of particles in suspension:

$$\left(\frac{(6\ x\ Polymer\ Weight\ (g))}{(3.14\ x\ Polymer\ Density\left(\frac{g}{cm^3}\right)\ x\ NP\ Diameter\ (\mathrm{um})^3}\right) x\ 10^{12} \quad \text{(Equation 2)}$$

Calculating the number of maleimide molecules in suspension:

$$\left(\frac{Polymer\ Mass\ (g)}{Polymer\ Molecular\ Weight\ \left(\frac{g}{mol}\right)}\right) x\ Avogadro's\ Number \quad \text{(Equation 3)}$$

Calculating the number of theoretical maleimide molecules per NP:

$$\frac{Number\ of\ Maleimide\ Molecules}{Number\ of\ Particles\ in\ Suspension} \quad \text{(Equation 4)}$$

Calculation of theoretical ligands per NP:

Theoretical number of maleimide molecules/NP x CE% (Equation 5)

Calculation of ligand availability (%):

$$\frac{Quantified\ ligands}{Theoretical\ number\ of\ ligands}\ x\ 100 \quad \text{(Equation 6)}$$

Cysteine assay protocol and calculation (For Table S3):

NP were conjugated with x5 molar excess of L-Cysteine (Sigma Aldrich, MW=175.63 g/mol) in comparison to maleimide content, for 2h in PBS and at R.T. under spinning conditions. Then, the NP solution was spun down via centrifugation (Eppendorf Microcentrifuge 5415 R Sigma-Aldrich) for 20 min at 16.1 x g (rcf) at 20°C leading to a NP pellet formation. The supernatant was collected, and the process was repeated on the supernatant for 2 times more until no pellet was observed. The negative control consisted of PLGA-PEG NP (without maleimide) undergoing the conjugation process and centrifugation steps identically to the test NP. The final supernatant solutions were analyzed using Ellman's test as per manufacturer's instructions[8]. Each sample was then analyzed using a NanoDrop Spectrophotometer at 412 nm and using the molar extinction coefficient of TNB (14,150 $M^{-1}cm^{-1}$). The conjugation efficiency was calculated as per Equation 1 in Supplementary Information.

Supplementary information and figures

Nanoparticle characterization
PLGA-PEG (PEG_{5k}) NPs

Please note that the PLGA-PEG 20% Maleimide formulation was formulated on a different day to the rest of the PLGA-PEG (PEG_{5k}) formulations.

Table S1. Analysis of the hydrodynamic radius (diameter nm) and polydispersity index (PdI) by Dynamic Light Scattering and zeta potential (ZP, mV) using a Zetasizer Nano ZS (Malvern Panalytical) at 25°C in miliQ water pH 7.0 for the PLGA-PEG (PEG_{5k}) NP formulations (a) before conjugation, (b) immediately after conjugation and (c) 7 days after conjugation with functional ligands (docking strands). The diameter is given as the z-average. The standard deviation (+/-) for 3 repeats is given. See Experimental Section – Nanoparticle Formulation for details on both maleimide and control NP formulations.

a)

Formulation	Diameter (nm)	PdI	Z-average (mV)
PLGA-PEG (control) 1	89.4 +/- 0.5	0.241 +/- 0.010	-20.5 +/- 0.4
PLGA-PEG 10% Maleimide	98.4 +/- 0.7	0.240 +/- 0.003	-23.7 +/- 0.1
PLGA-PEG 20% Maleimide	108.3 +/- 0.4	0.105 +/- 0.012	-16.6 +/- 0.6
PLGA-PEG 30% Maleimide	97.3 +/- 0.6	0.201 +/- 0.018	-26.4 +/- 0.3
PLGA-PEG 50% Maleimide	101.9 +/- 2.0	0.194 +/- 0.030	-25.6 +/- 0.6
PLGA-PEG 70% Maleimide	108.3 +/- 0.8	0.147 +/- 0.019	-26.0 +/- 0.5
PLGA-PEG 100% Maleimide	105.3 +/- 0.5	0.153 +/- 0.017	-21.6 +/- 0.7

b)

Formulation	Diameter (nm)	PdI	Z-average (mV)
PLGA-PEG (control) 1	86.5 +/- 0.7	0.155 +/- 0.005	-10.2 +/- 0.3
PLGA-PEG 10% Maleimide	86.5 +/- 0.3	0.162 +/- 0.016	-10.4 +/- 0.4
PLGA-PEG 20% Maleimide	111.2 +/- 0.4	0.068 +/- 0.033	-23.0 +/- 0.2
PLGA-PEG 30% Maleimide	83.0 +/- 0.1	0.099 +/- 0.016	-15.8 +/- 0.5
PLGA-PEG 50% Maleimide	87.9 +/- 0.7	0.078 +/- 0.010	-21.3 +/- 0.9
PLGA-PEG 70% Maleimide	99.1 +/- 0.5	0.052 +/- 0.014	-21.7 +/- 0.3
PLGA-PEG 100% Maleimide	116.0 +/- 1.0	0.190 +/- 0.001	-27.8 +/- 0.7

c)

Formulation	Diameter (nm)	PdI	Z-average (mV)
PLGA-PEG (control) 1	97.6 +/- 0.5	0.183 +/- 0.014	-7.7 +/- 0.4
PLGA-PEG 10% Maleimide	86.7 +/- 1.1	0.151 +/- 0.013	-9.3 +/- 0.9
PLGA-PEG 20% Maleimide	119.4 +/- 1.1	0.086 +/- 0.048	-16.9 +/- 0.3
PLGA-PEG 30% Maleimide	83.3 +/- 1.0	0.086 +/- 0.021	-14.6 +/- 0.4
PLGA-PEG 50% Maleimide	87.0 +/- 0.7	0.066 +/- 0.005	-20.0 +/- 0.5
PLGA-PEG 70% Maleimide	97.9 +/- 0.5	0.056 +/- 0.004	-24.9 +/- 1.1
PLGA-PEG 100% Maleimide	124.6 +/- 3.4	0.241 +/- 0.033	-31.2 +/- 0.7

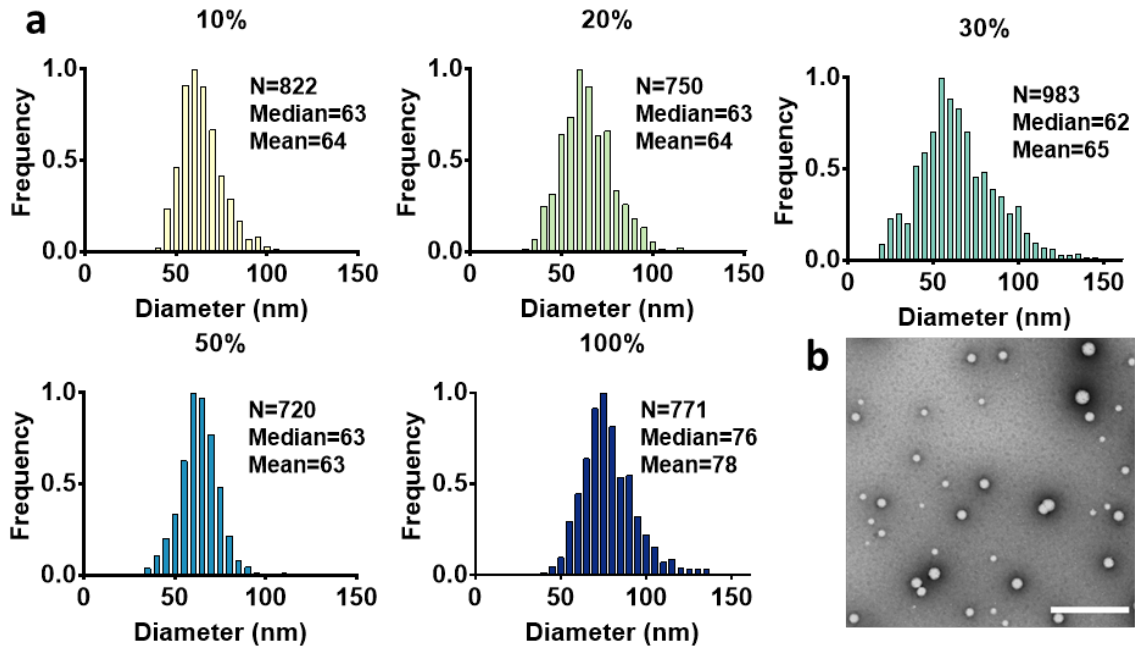

Fig. S1. (a) Normalized frequency histograms of NP diameter (nm) from TEM images, of ligand-conjugated PLGA-PEG (PEG_{5k}) NPs with varying maleimide content (10, 20, 30, 50 and 100%). The number of NPs analyzed (N), and median and mean diameters are given for each. Bin widths=5 nm. (b) TEM image representative of a 10% maleimide formulation (scale bar 500 nm).

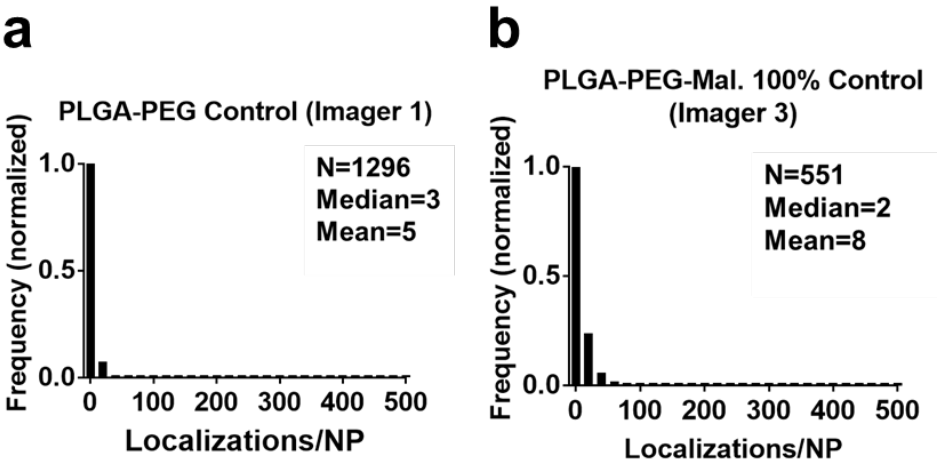

Fig. S2. (a) Normalized frequency histograms of DNA-PAINT localizations for control PLGA-PEG (PEG_{5k}) NPs (with no maleimide content) after imaging with imager strand 1, and (b) for PLGA-PEG (PEG_{5k}) NPs with 100% maleimide content after conjugation to functional ligands (docking strands) and imaging with imager strand 3 (non-complementary pairing). The number of nanoparticles analyzed (N), the median and mean number of localizations are also shown. The data were analyzed using Matlab Software.

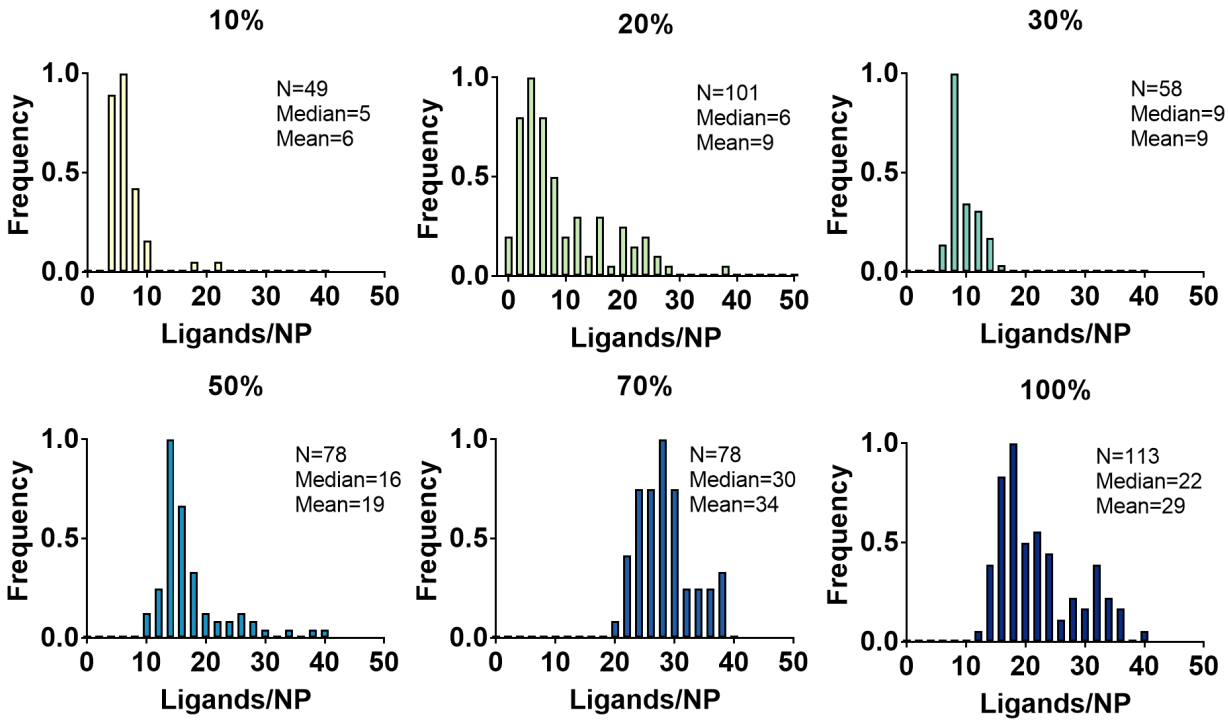

Fig. S3. (a) Normalized frequency histograms of number of functional ligands (docking strands)/NP as quantified by qPAINT for PLGA-PEG (PEG_{5k}) NPs with varying maleimide contents (10-100%). The number of nanoparticles analyzed (N), the median and mean number of localizations are also shown. Bin width=2 nm. The data were analyzed using Matlab Software.

Table S2. Properties of PLGA-PEG NPs with varying maleimide content and spacer PEG length

Formulation	Diameter by TEM (nm)	Theoretical maleimide molecules/NP	CE%	Theoretical ligand number/NP	Quantified ligands by qPAINT	Ligand availability (%)
PLGA-PEG-Mal. 10% (PEG_{5k})	64 +/- 12	307	25	77	6	8
PLGA-PEG-Mal. 20% (PEG_{5k})	64+/- 15	612	21	129	8	6
PLGA-PEG-Mal. 30% (PEG_{5k})	65 +/- 23	962	31	293	9	2
PLGA-PEG-Mal. 10% (PEG_{1k})	77 +/- 25	529	38	203	42	21
PLGA-PEG-Mal. 20% (PEG_{1k})	76 +/- 25	1025	35	359	54	15
PLGA-PEG-Mal. 30% (PEG_{1k})	78 +/- 29	1630	70	1141	54	5

For calculations of theoretical maleimide molecules/NP, CE%, theoretical ligand number/NP and ligand availability (%) see Experimental section.

Table S3. Conjugation efficiency (CE%) of PLGA-PEG NP formulations with varying maleimide content and spacer PEG lengths after conjugation with L-Cysteine, to study maleimide availability. For protocol and calculations see Experimental section.

Formulation	Cysteine CE (%)
PLGA-PEG-Mal. 10% (PEG_{5k})	46
PLGA-PEG-Mal. 20% (PEG_{5k})	41
PLGA-PEG-Mal. 30% (PEG_{5k})	49
PLGA-PEG-Mal. 10% (PEG_{1k})	47
PLGA-PEG-Mal. 20% (PEG_{1k})	55
PLGA-PEG-Mal. 30% (PEG_{1k})	65

Nanoparticle characterization

PLGA PEG NPs (PEG_{1K})

Please note that the PLGA-PEG 20% Maleimide formulation was formulated on a different day to the rest of the PLGA-PEG (PEG_{1K}) formulations.

Table S4. Analysis of the hydrodynamic radius (diameter nm) and polydispersity index (PdI) by Dynamic Light Scattering and zeta potential (ZP, mV) using a Zetasizer Nano ZS (Malvern Panalytical) at 25°C in miliQ water pH 7.0 for the PLGA-PEG (PEG_{1k}) NP formulations (a) before conjugation, (b) immediately after conjugation and (c) 7 days after conjugation with functional ligands (docking strands). The diameter is given as the z-average. The standard deviation (+/-) for 3 repeats is given. The control formulations contain no maleimide, but the same ratio of PEG_{5k} vs PEG_{1k} (see Experimental Section – Nanoparticle Formulation).

a)

Formulation	Diameter (nm)	PdI	Z-average (mV)
PLGA-PEG 10% control	103.6 +/- 0.4	0.130 +/- 0.017	-29.9 +/- 0.6
PLGA-PEG 10% Maleimide	152.1 +/- 3.8	0.141 +/- 0.058	-37.5 +/- 0.5
PLGA-PEG 20% control	114.2 +/- 1.9	0.073 +/- 0.040	-18.9 +/- 0.1
PLGA-PEG 20% Maleimide	183.9 +/- 2.7	0.108 +/- 0.017	-25.4 +/- 0.5
PLGA-PEG 30% control	123.0 +/- 2.1	0.197 +/- 0.031	-37.1 +/- 1.4
PLGA-PEG 30% Maleimide	161.4 +/- 9.7	0.157 +/- 0.056	-28.7 +/- 0.6

b)

Formulation	Diameter (nm)	PdI	Z-average (mV)
PLGA-PEG 10% control	117.0 +/- 0.9	0.101 +/- 0.018	-30.3 +/- 0.3
PLGA-PEG 10% Maleimide	165.9 +/- 6.4	0.071 +/- 0.050	-30.3 +/- 0.7
PLGA-PEG 20% control	113.4 +/- 1.6	0.094 +/- 0.017	-20.3 +/- 0.7
PLGA-PEG 20% Maleimide	191.3 +/- 4.5	0.108 +/- 0.029	-31.9 +/- 0.5
PLGA-PEG 30% control	120.9 +/- 1.6	0.142 +/- 0.031	-26.0 +/- 0.4
PLGA-PEG 30% Maleimide	156.9 +/- 4.9	0.157 +/- 0.056	-31.0 +/- 0.2

c)

Formulation	Diameter (nm)	PdI	Z-average (mV)
PLGA-PEG 10% control	116.5 +/- 2.4	0.087 +/- 0.057	-23.7 +/- 0.4
PLGA-PEG 10% Maleimide	164.6 +/- 2.0	0.164 +/- 0.059	-26.4 +/- 0.9
PLGA-PEG 20% control	115.6 +/- 0.8	0.101 +/- 0.029	-20.5 +/- 0.7
PLGA-PEG 20% Maleimide	184.5 +/- 3.6	0.109 +/- 0.013	-30.7 +/- 0.7
PLGA-PEG 30% control	124.3 +/- 1.9	0.095 +/- 0.038	-21.6 +/- 0.3
PLGA-PEG 30% Maleimide	158.8 +/- 1-6	0.090 +/- 0.034	-25.0 +/- 0.4

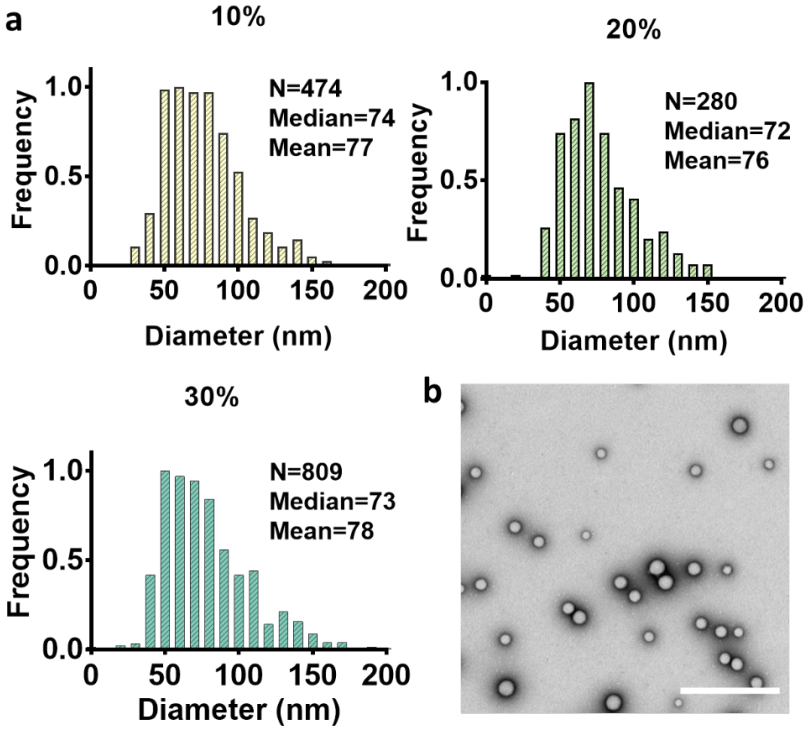

Fig. S4. (a) Normalized frequency histograms of NP diameter (nm) from TEM images, of ligand-conjugated PLGA-PEG NPs (PEG_{1k}) with varying maleimide content (10, 20, 30%). The number of NPs analyzed (N), and median and mean diameters are given for each. Bin widths=10 nm. (b) TEM image representative of a 10% maleimide formulation (scale bar 500 nm).

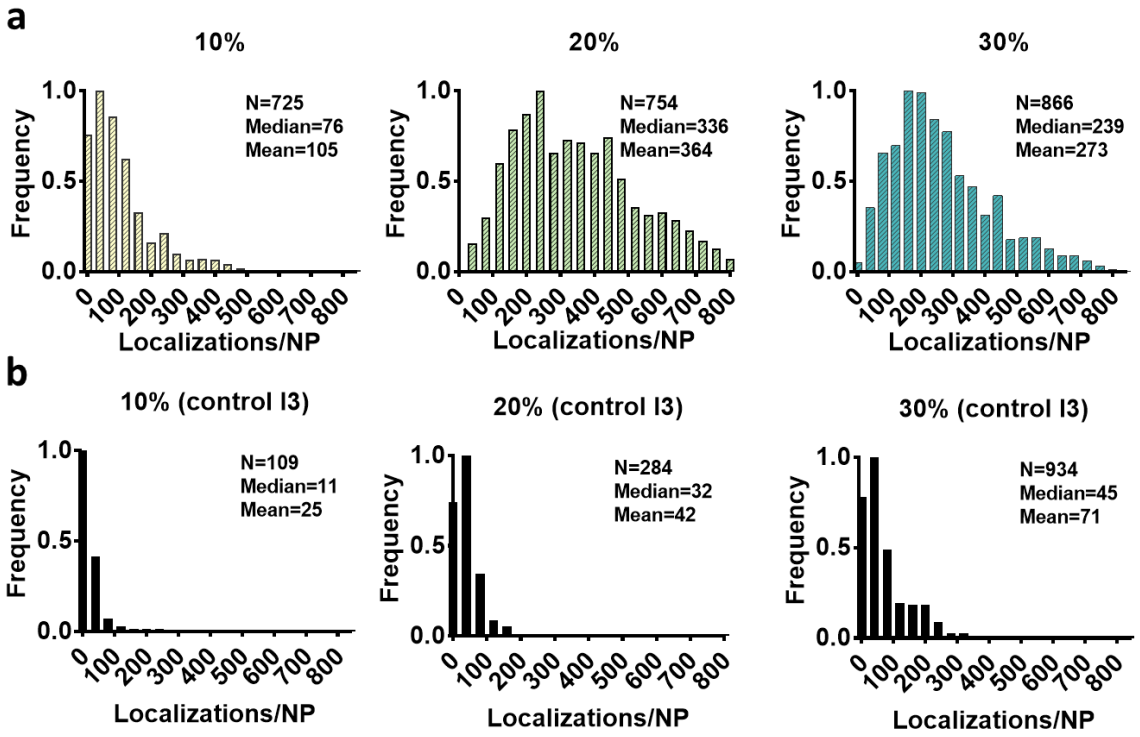

Fig. S5. (a) Normalized frequency histograms of DNA-PAINT localizations for PLGA-PEG (PEG_{1k}) NPs with varying maleimide contents (10, 20, 30%) after conjugation to functional ligands (docking strands) and imaging with imager strand 3 (correct pairing). (b) Normalized frequency histograms of DNA-PAINT localizations for PLGA-PEG (PEG_{1k}) NPs with varying maleimide contents (10, 20, 30%) after conjugation to functional ligands (docking strands) and imaging with imager strand 3 (non-complementary pairing). Bin width=40 nm. The number of nanoparticles analyzed (N), the median and mean number of localizations are also shown. The data were analyzed using Matlab Software.

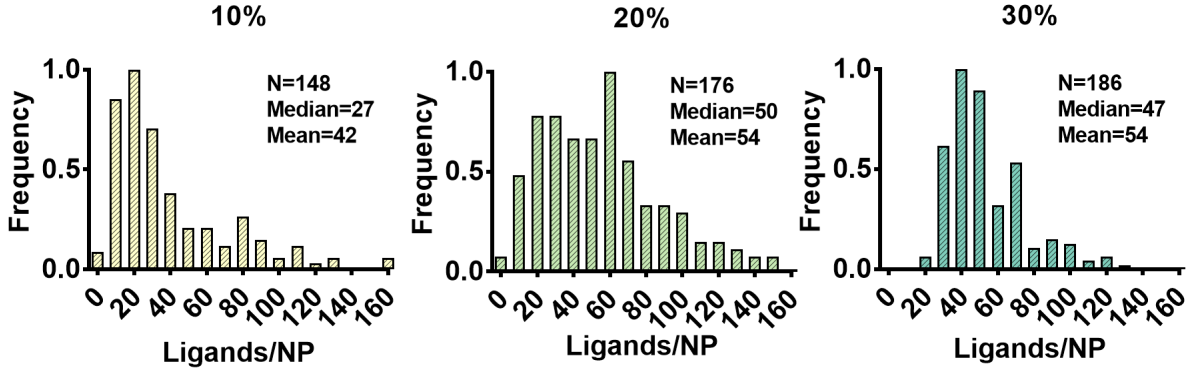

Fig. S6. (a) Normalized frequency histograms of number of available ligands/NP as quantified by qPAINT for PLGA-PEG (PEG_{1k}) NPs with varying maleimide contents (10, 20, 30%). The number of nanoparticles analyzed (N), the median and mean number of localizations are also shown. Bin width=10 nm. The data were analyzed using Matlab Software.

(1) Barichello, J. M.; Morishita, M.; Takayama, K.; Nagai, T. Encapsulation of Hydrophilic and Lipophilic Drugs in PLGA Nanoparticles by the Nanoprecipitation Method. *Drug Development and Industrial Pharmacy* **1999**, *25* (4), 471–476. https://doi.org/10.1081/DDC-100102197.
(2) Andrian, T.; Delcanale, P.; Pujals, S.; Albertazzi, L. Correlating Super-Resolution Microscopy and Transmission Electron Microscopy Reveals Multiparametric Heterogeneity in Nanoparticles. *Nano Letters* 9.
(3) Invitrogen Molecular Probes. Thiol-Reactive Probes. 2006.
(4) Delcanale, P.; Miret-Ontiveros, B.; Arista-Romero, M.; Pujals, S.; Albertazzi, L. Nanoscale Mapping Functional Sites on Nanoparticles by Points Accumulation for Imaging in Nanoscale Topography (PAINT). *ACS Nano* **2018**, *12* (8), 7629–7637. https://doi.org/10.1021/acsnano.7b09063.
(5) Delcanale, P.; Albertazzi, L. DNA-PAINT Super-Resolution Imaging Data of Surface Exposed Active Sites on Particles. *Data in Brief* **2020**, *30*, 105468. https://doi.org/10.1016/j.dib.2020.105468.
(6) Andrian, T.; Delcanale, P.; Pujals, S.; Albertazzi, L. Correlating Super-Resolution Microscopy and Transmission Electron Microscopy Reveals Multiparametric Heterogeneity in Nanoparticles. *Nano Lett.* **2021**, *21* (12), 5360–5368. https://doi.org/10.1021/acs.nanolett.1c01666.
(7) Spherotech Inc. Particle characteristics https://www.spherotech.com/particle.html (accessed 2020 -07 -20).
(8) Ellman's Reagent Instructions https://assets.thermofisher.com/TFS-Assets/LSG/manuals/MAN0011216_Ellmans_Reag_UG.pdf (accessed 2020 -10 -05).